



# PSO-Based Initial SOC and Capacity Optimization for Stationary Energy Storage Systems in DC Electric Railway System

Kisuk Kim<sup>1</sup> · Jaewon Kim<sup>2</sup> · Changmu Lee<sup>2</sup> · Joorak Kim<sup>2</sup> · Hansang Lee<sup>3</sup> 

Received: 16 November 2020 / Revised: 2 April 2021 / Accepted: 6 April 2021 / Published online: 3 May 2021  
© The Korean Institute of Electrical Engineers 2021, corrected publication 2021

## Abstract

This paper presents an PSO-based optimization methodology for estimating the capacities and initial SOC of an energy storage systems (ESSs) in a DC electric railway system. The proposed method calculates the optimal solution using the missing capacity caused by the limited storage capacity. The missing capacity can be estimated through continuous-powerflow analysis. In many previous studies, capacities was calculated by assuming the each ESS as an independent device. However, since each storage device affects the charging and discharging operation of each other, this assumption might affect the convergence characteristics. In this paper, to solve this problem, the missing capacity of the ESS at both sides is reflected by using the relating coefficient derived based on the electrical distance between storage devices. The case studies show that the most efficient operation without missing capacity is possible under the derived capacities and initial SOC.

**Keywords** DC electric railway system (DC ERS) · Regenerative energy · Energy storage system (ESS) · Initial SOC · Efficiency

## 1 Introduction

In response to rapid climate change, the international community is obligated to reduce greenhouse gas emission through the Paris Agreement in COP21, and the transportation/transport sector is also making efforts to develop technologies and systems for this. As the share of energy consumed by railroad transportation is high among all means of

transportation, it is a situation that should contribute to the reduction of greenhouse gases. Electricity rates are expected to rise due to the shift in the energy paradigm into renewable generation, and the operating costs in railway institutions are also expected to be increased dramatically. In response to these climate agreements and energy paradigm shifts, railway engineers have conducted researches to improve the efficiency of individual part and to achieve energy-efficient operational strategies. Among them, with regard to rational energy consumption, the most active research is being conducted on the optimal design and operation of energy storage system (ESS) which can directly contribute to the proper operation of regenerative energy.

An energy storage system is a technology that can improve added value or operational efficiency through the interval between the time of production and consumption of electricity, and various studies on optimal utilization and operation plans are being conducted based on high utility. It can be used as a means of securing the supply reliability of renewable power generation with high volatility, and research on optimal capacity calculation and control/operation methods for the purpose of realizing supply and demand stabilization through short-term fluctuation suppression and long-term fluctuation compensation has been carried out [1–3]. In addition, various methodologies for calculating the

✉ Hansang Lee  
hslee@semyung.ac.kr

Kisuk Kim  
kks1213@korea.ac.kr

Jaewon Kim  
youngkjw@krri.re.kr

Changmu Lee  
cmlee@krri.re.kr

Joorak Kim  
jrkim@krri.re.kr

<sup>1</sup> School of Electrical Engineering, Korea University, Seoul, Korea

<sup>2</sup> Korea Railroad Research Institute, Uiwang, Korea

<sup>3</sup> Department of Electrical Engineering, Semyung University, Jecheon, Korea

optimal capacity of ESS at various sites within the power system, such as capacity calculation for minimizing operating costs for the same power usage at the microgrid scale, have been proposed [4–7].

In the case of the railway system, the focus is on the proper use of regenerative energy as a means for system efficiency. The regenerative energy generated by the braking vehicle is consumed by nearby accelerating vehicles, but more than 60% of the energy is not utilized and is consumed as heat through the resistor. This means that the energy efficiency of the railroad system can be remarkably improved by only recycling the waste regenerative energy. For this reason, a number of studies have been conducted on the design, control, and operation of devices that enable the use of regenerative energy such as stationary storage devices, on-board storage devices, and regenerative inverters [8–11]. Most studies have been conducted on the energy saving effect analysis based on the characteristics of the route (the topographical structure of the track, the distance between stations, the location of the substation, etc.), the driving conditions of the vehicle, the capacity calculation, location selection of the regenerative energy utilization technology. The application of the railway system of ESS is typically applied for the purpose of improving efficiency through reuse of regenerative energy, reducing peak power, and diversifying supply energy sources. Researches about the effect of improving efficiency is self-operation of regenerative energy considering the on-board storage device [10, 11], optimal charge/discharge algorithm for stationary storage device [12], optimal capacity calculation for each device [12], and peak power reduction for high load times [13], etc. are ongoing. These studies deal with comprehensive issues on the energy management of the system as a whole, but do not clearly present detailed operation strategies of the energy storage device itself. In addition, researches on the use of energy storage devices are being conducted in order to seamlessly link the railway system with renewable power sources [14, 15], but the energy storage devices in this case are mainly studied in terms of control rather than in terms of operation.

As mentioned above, in the existing studies, a detailed discussion on setting the operating point or effective operating range of the energy storage device itself has not been carried out beyond the system point of view. Initial operation point setting and effective operation range setting maximizes the availability of designed storage capacity and maintains high SOC by eliminating the existence of a point in time when regenerative energy cannot be stored due to the buffered state of ESS or supply by complete discharge is impossible. Its purpose is to improve the operating life and economic efficiency of ESS through the use of. Therefore, in this paper, an initial optimal operating point setting and an effective operating range calculation algorithm based on particle swarm optimization (PSO) are presented. In addition,

we proved that the algorithm is valid for the ESS with the optimized storage capacity assumed for the substation of a specific route.

This paper deals with the method for power and storage capacity estimation of ESSs in Chapter 2, and presents an algorithm for calculating the initial operating point recommendation in Chapter 3. In Chapter 4, the effectiveness of the proposed algorithm was verified for the actual running route.

## 2 Optimal Initializing of ESS in DC Electric Railway System

The kinetic energy of a railway vehicle accelerated through the consumption of electric energy is converted into electric energy during the braking process by the application of the electric braking system and supplied to the contact wire as shown in Fig. 1. From the Eq. (1) about the vehicle power, regenerative power is generated in the process of implementing a deceleration over air and mechanical resistive force. Depending on the conditions of route, about normally 40–60% of regenerative energy is used to be consumed for acceleration of vehicle(s) which is/are operating at near location.

$$P_{tractive} = m_{veh} a_{eff} v_{veh} + C_a \rho A v_{veh}^3 + \mu_k m g v_{veh} \quad (1)$$

where  $P_{tractive}$ : traction power of vehicle,  $m_{veh}$ : mass of vehicle,  $a_{eff}$ : effective acceleration of vehicle,  $v_{veh}$ : velocity of vehicle,  $C_a$ : coefficient for resistive force,  $\rho$ : air density,  $A$ : cross-sectional area of vehicle,  $\mu_k$ : coefficient for kinetic friction.

However, the generated regenerative power cannot be consumed entirely for several physical reasons. Firstly, because the regenerative power from the braking vehicle and the power consumption pattern of the starting vehicle are opposite, all the generated regenerative power cannot be

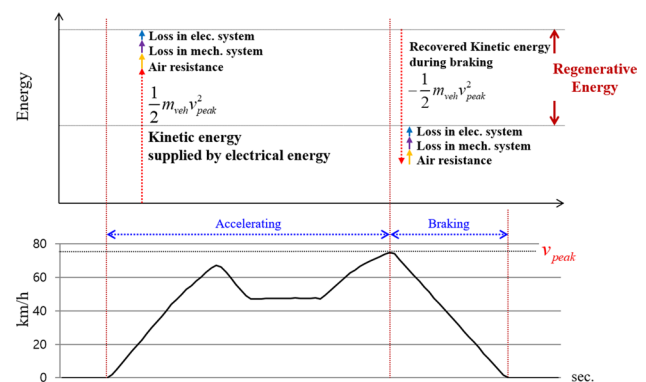


Fig. 1 Definition of regenerative power

consumed only by starting the vehicle. At the first term in Eq. (1) containing the relationship with the vehicle speed, it can be seen that the magnitude and the sign of the power are determined by vehicle speed and acceleration, respectively. That is, even if the timing of braking and starting is exactly matched, it means that only 50% of regenerative power can be consumed.

Secondly, the remaining regenerative power after consuming by some accelerating vehicles cannot be re-supplied back to the grid because the DC electric railway system is supplied by a unidirectional diode rectifier. So the DC railway system operates to consume the remaining energy as heat through a regenerative resistor device in order to maintain the power balance when the regenerative power is greater than the power consumption as shown in Fig. 2. Through this operation, the dissipation of energy which can be recycled and the unnecessary power consumption such as air-conditioning to reduce temperature rise in the tunnel and platform are usually occurred. Therefore, if unnecessary energy consumption by the regenerative resistor is eliminated by resolving the discrepancy between the amount of regenerative power and the demand point of the railway system, the electric energy which is supplied from the grid to implement the same operation can be minimized.

As mentioned before, efficiency improvement by resolving the discrepancy between the total power demand and the amount of regenerative power can be implemented through the operation of ESS as shown in Fig. 2. Since the amount of energy to be handled by energy storage at each substation is different according to the characteristics of the route, such as the topographical condition of the track, the distance between substations, headway, etc., the reference voltage set, which determines charging, holding, or discharging operation, and the required power and storage capacities are estimated differently. The optimal storage capacity calculation for improving efficiency is performed through the following process.

### 2.1 System Matrix

Analysis of the DC electric railway system considering ESS is performed based on the conductance matrix as shown in Eq. 2. Based on the specific operation mode of the ESS, the purpose of this analysis is to calculate the value of the additional current in the charging or discharging mode. The calculated current value is used to determine the operating capacity of the ESS in the charging or discharging mode as shown in Eqs. 3.

$$[Y]^t \begin{bmatrix} V_{sub1}^t \\ \vdots \\ V_{subn}^t \\ V_{cat1}^t \\ \vdots \\ V_{rail1}^t \\ \vdots \end{bmatrix} = \begin{bmatrix} I_{sub1} + I_{ESS1}^t \\ \vdots \\ I_{subn} + I_{ESSn}^t \\ -I_{veh1}^t \\ \vdots \\ I_{veh1}^t \\ \vdots \end{bmatrix}$$

where  $[Y]^t$ : system conductance matrix at  $t$ ,  $V_{sub i}^t$ : catenary voltage of  $i$ th substation at  $t$ ,  $I_{sub i}$ : Norton equivalent current of  $i$ th substation,  $V_{cat j}^t$ : catenary voltage of  $j$ th vehicle at  $t$ ,  $V_{rail j}^t$ : rail voltage of  $j$ th vehicle at  $t$ ,  $I_{veh j}^t$ : vehicle current of  $j$ th vehicle at  $t$ ,  $I_{ESS i}^t$ : ESS current at  $i$ th substation at  $t$ .

$$P_{ESSi}^t = V_{subi}^t \cdot I_{ESSi}^t \tag{3}$$

where  $P_{ESS i}^t$ : charging or discharging capacity of  $i$ th ESS

### 2.2 Charging Mode Determination of ESSs

The diode rectification type train substation can be expressed as an equivalent power source of voltage source and internal resistance. Here, the internal voltage of the equivalent model is called the no-load voltage, and is designed to be 1650 V in the case of the metropolitan area and 1620 V in the case of a local metropolis, in Korea. That is, since the power flow in the

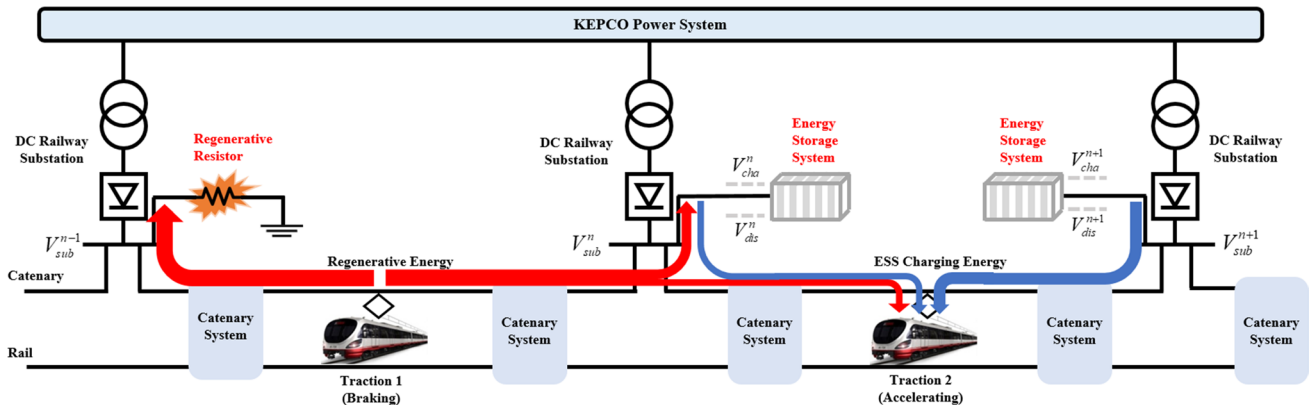


Fig. 2 Conceptual energy flow in DC electric railway system

reverse direction is not allowed, the substation voltage above the no-load voltage cannot exist under the supply condition. However, substation voltages higher than the no-load voltage frequently occur, and it is widely known that the cause of this is the regenerative power from the braking vehicle. Based on the understanding of this simple phenomenon, the ESS should be set to detect and charge regenerative power with voltage conditions above no-load voltage, and the charging capacity should be a operation equal to the charging current that prevents the substation voltage from exceeding the no-load voltage. Defining the variable for the operation mode of the  $i^{\text{th}}$  substation storage device at time  $t$  is  $S_{ESSi}^t$ , the charging operation can be expressed as Eq. (4).

$$S_{ESSi}^t = \eta (V_{subi}^t \geq V_{noload}) \tag{4}$$

where  $\eta$ : Power Conversion Efficiency of ESS.

### 2.3 Discharging mode of ESSs

The total amount of the stored regenerative energy must be resupplied when the grid needs it. In general, through resupplying at the time when it has the highest usefulness, the energy stored in the ESS gives effects to increase grid operation efficiency or reduce cost. In the case of the railway system, the stored regenerative energy is used to maximize effects to reduce the demand of the substation or lower the peak power.

In fact, determining the discharging operations of ESS in a railroad system is complicated enough that it cannot be determined through numerical analysis like a powerflow analysis. The discharging operation of an ESS cannot be deterministically because it is affected by various variables such as the driving state of the neighbor vehicles, the voltage of the other substation, and the operation mode of the other ESS. This process will be mentioned in the optimization process in Sect. 2.4. However, it must be strongly noticed that the constraints as shown in Eq. (5) about clearing accumulated energy must be satisfied, when considering the repetitively operational characteristic of the railway system. The value of the ESS operation mode variable in holding or discharging is shown in Eq. 6. And, the cumulated energy in the ESS is updated using Eq. (7) at every time step.

$$\sum_{t=1}^{headway} S_{ESSi}^t \cdot P_{ESSi}^t = 0 \tag{5}$$

$$\begin{aligned} S_{ESSi}^t &= 0 \text{ (holding)} \\ &= \frac{1}{\eta} \text{ (discharging)} \end{aligned} \tag{6}$$

$$E_{ESSi}^t = E_{ESSi}^{t-1} + S_{ESSi}^t \cdot P_{ESSi}^t \tag{7}$$

where  $E_{ESSi}^t$ : cumulated energy in  $i^{\text{th}}$  ESS at time  $t$ .

### 2.4 Optimization for Storage Capacity and Initial SOC

The initial SOC optimization of an ESS in a railway substation consists of two processes: minimizing the power supply to the substation under peak headway operating conditions that require a larger storage capacity, and minimizing the depth of discharge(DOD) of the ESS under off-peak headway conditions. In other words, it is a process of minimizing the operating cost and life cost of ESSs, and it is performed using the PSO algorithm. The objective function and constraints for each optimization process are as follows.

$$\min \left\{ \sum_{t=1}^{headway} P_{SUBi}^t \right\} \tag{8}$$

$$\min \left\{ \sum_{t=1}^{headway} DOD_{ESSi}^{\max} \right\} \tag{9}$$

subject to  $V_{SUBi}^t \leq V_{no-load} (i = 1, 2, \dots, n)$

$$\sum_{t=1}^{headway} S_{ESSi}^t \cdot P_{ESSi}^t = 0 \tag{10}$$

Main terms for PSO are presented as below:

*Particle* is defined as the set of initial SOC( $IS_i$ ) as shown in Eq. (11) with assumption of  $n$  substations. Each initial SOC value is chosen randomly.

$$IS = [IS_1 \ IS_2 \ \dots \ IS_i \ \dots \ IS_n]^T \tag{11}$$

*Population* ( $n_p$ ) is the number of Particle sets in the swarm matrix.

*Swarm matrix* is the matrix with dimension of  $n$  by  $PO$  at  $m^{\text{th}}$  iteration as shown in Eq. (12).

$$M_{swarm}^m = \begin{bmatrix} IS_{1,1}^m & \dots & IS_{i,1}^m & \dots & IS_{n_p,1}^m \\ \vdots & \ddots & \vdots & \ddots & \vdots \\ IS_{1,j}^m & \dots & IS_{i,j}^m & \dots & IS_{n_p,j}^m \\ \vdots & \ddots & \vdots & \ddots & \vdots \\ IS_{1,n}^m & \dots & IS_{i,n}^m & \dots & IS_{n_p,n}^m \end{bmatrix} \tag{12}$$

*Global best* is the best  $IS$  set at  $m^{\text{th}}$  iteration as shown in Eq. (13).

$$IS_g^* = [IS_{1,g}^m \ IS_{2,g}^m \ \dots \ IS_{i,g}^m \ \dots \ IS_{n,g}^m]^T \tag{13}$$

The initial SOC and capacity update is performed using the missing capacity calculated in the previous step. Here, the missing capacity refers to the amount of regenerative

energy that cannot be stored or discharged because of the limited storage capacity. Equations (14) and (15) show the missing capacities,  $MC_{pESSi}^m$  and  $MC_{nESSi}^m$ . Here,  $\lambda_{pi}^t$  becomes 1 when 100% of SOC and charging mode of ESS and  $\lambda_{ni}^t$  becomes  $-1$  at vice versa.

$$MC_{pESSi}^m = \sum_{t=1}^{headway} \lambda_{pi}^t \cdot (E_{mi}^t - S_{ESSi}^t \cdot P_{ESSi}^t) \tag{14}$$

$$MC_{nESSi}^m = \sum_{t=1}^{headway} \lambda_{ni}^t \cdot (-S_{ESSi}^t \cdot P_{ESSi}^t - (E_{maxi} - E_{mi}^t)) \tag{15}$$

where  $MC_{pESSi}^m$ : total amount of energy not charged in  $i$ th ESS at step  $m$ ,  $MC_{nESSi}^m$ : total amount of energy not discharged in  $i$ th ESS at step  $m$ .

Using the missing capacity calculated in the previous step, the initial SOC and storage capacity can be updated. The charge/discharge operation of each energy storage device is not independent. Since it is connected to one rigid conductor in parallel, the charge/discharge mode or charge/discharge capacity may vary depending on the operation of an adjacent storage device. That is, by the charging operation of the adjacent storage device, the requested capacity to be charged may be reduced. This means that when updating the capacity and initial operating point of a specific storage device, it is necessary to consider the missing capacity of the storage devices located at both sides in the previous step. The storage capacity and initial SOC are updated based on Eqs. (16)–(19).

$$CoSTO_{pESSi}^m = \alpha \cdot MC_{pESSi}^m - \beta \cdot MC_{pESSi-1}^m - \gamma \cdot MC_{pESSi+1}^m \tag{16}$$

$$CoSTO_{nESSi}^m = \alpha \cdot MC_{nESSi}^m - \beta \cdot MC_{nESSi-1}^m - \gamma \cdot MC_{nESSi+1}^m \tag{17}$$

where  $CoSTO$ : correction capacity considering storage devices on both sides,  $\alpha, \beta, \gamma$ : relating coefficients

$$STO_i^m = STO_i^{m-1} + CoSTO_{pESSi}^m - CoSTO_{pESSi}^m \tag{18}$$

where  $STO_i^m$ : storage capacity of  $i$ th ESS at step  $m$

$$IS_{ij}^m = \frac{IS_{ij}^{m-1} \cdot STO_i^{m-1} + CoSTO_{pESSi}^m}{STO_i^{m-1} + CoSTO_{pESSi}^m + CoSTO_{nESSi}^m} \tag{19}$$

Figure 3 shows the entire process for estimating the optimal storage capacity and initial SOC described above.

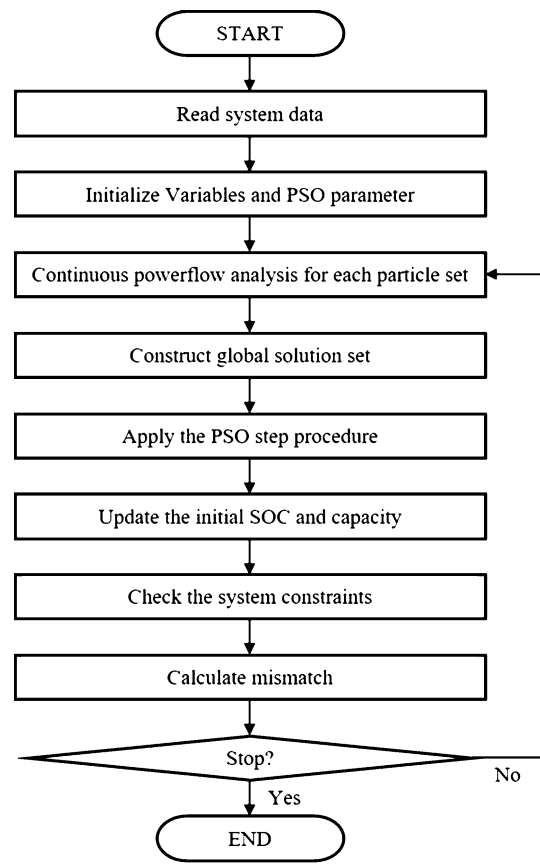


Fig. 3 Flowchart for PSO-based storage and initial SOC optimization algorithm

### 3 Case Studies

In order to verify the effectiveness of the proposed algorithm, the algorithm was applied to the actual route. The system information for the route and the result of applying the algorithm are as follows.

#### 3.1 System Data

In order to effectively show the application effect of the proposed algorithm, the Seoul Metro Line 8, which has the smallest number of substations, is chosen among the domestic DC electric railway lines. The electrical characteristics and route information of Line 8 are presented in Table 1.

#### 3.2 Optimization Results

Table 2 shows the power and storage capacity results of each storage device derived by the proposed algorithm. It can be seen that the power capacity is dependent on the peak

**Table 1** Electrical characteristics and route information of Seoul Metro Line 8

Category	Data	Values
Electrical Data	No-load voltage	1650 V
	Source impedance	0.02956 $\Omega$
	Catenary impedance	20.3 m $\Omega$ /km
	Rail impedance	0.464 m $\Omega$ /km
Structural Data	Location of Sub 1	2244 m
	Location of Sub 2	6951 m
	Location of Sub 3	12,026 m
	Location of Sub 4	16,063 m
	Location of Sub 5	19,902 m
Operational Data	Headway for peak	240 s
	# of vehicle for peak	16
	Headway for off-peak	480 s
	# of vehicle for off-peak	8

headway load condition where the vehicle running per unit time is larger. In other words, it means that there might be a high probability that more vehicles might regenerate or consume simultaneously. On the other hand, the required storage capacity is not highly correlated with vehicle operating conditions. For the higher number of driving vehicles, there might be more load candidates that can consume regenerative power. The results in Table 2 shows that the demand for operation of a storage device for handling regenerative energy might be rather reduced.

The design capacity is derived from the available capacity calculated from each load condition. In the case of a battery or supercapacitor type storage device, the ratio of the available capacity to the total capacity is 75%, because the operational range of the ESS internal voltage is limited to 50% of the maximum voltage.

**Table 2** Estimated power and storage capacity

ESS location	peak headway (240 s.)		off-peak headway (480 s.)		storage capacity design (kWh)
	power capacity (MW)	storage capacity (kWh)	power capacity (MW)	storage capacity (kWh)	
Sub 1	<b>1.283</b>	<b>22.27</b>	0.977	17.25	<b>29.70</b>
Sub 2	<b>1.197</b>	17.32	0.900	<b>20.38</b>	<b>27.18</b>
Sub 3	<b>1.279</b>	12.00	0.989	<b>18.60</b>	<b>24.81</b>
Sub 4	<b>1.345</b>	<b>13.09</b>	0.837	12.45	<b>17.45</b>
Sub 5	<b>0.993</b>	<b>18.95</b>	0.740	13.46	<b>25.27</b>

'Bold text' means the determined specification of each substation ESS

**Table 3** Optimal initial-SOC for peak headway condition

ESS location	Optimal initial SOC (%)
Sub 1	82.66
Sub 2	63.49
Sub 3	67.48
Sub 4	25.10
Sub 5	63.47

### 3.3 Peak Headway Condition

Table 3 shows the results of estimating the initial operating point based on the proposed algorithm under peak load operating conditions. As shown in Fig. 4, in the case of substations 1, 4, and 5, which determines designed capacity under peak headway condition, storage devices are operated in the full range of 25% and 100% with the initial SOC of 82.66%, 25.10%, and 63.47%, respectively. In addition, in the case of the storage devices of the substations 2 and 3, it can be seen that the DODs of storages is limited to 36.70% and 51.65% with the initial SOC of 63.49% and 67.48%, respectively.

### 3.4 Off-peak Headway Condition

Table 4 and Fig. 5 show the results of estimating the initial operating point and based on the proposed algorithm under peak load operating conditions. Storage devices in the substation 2 and 3 are operated in the full range of 25% and 100% with the initial SOC of 87.17% and 79.78%, respectively. And, the maximum DOD of the storages in the substations 1, 4, and 5 is calculated to be 41.91%, 28.68%, and 46.74% with the initial SOC of 92.65%, 28.89%, and 81.44%, respectively.

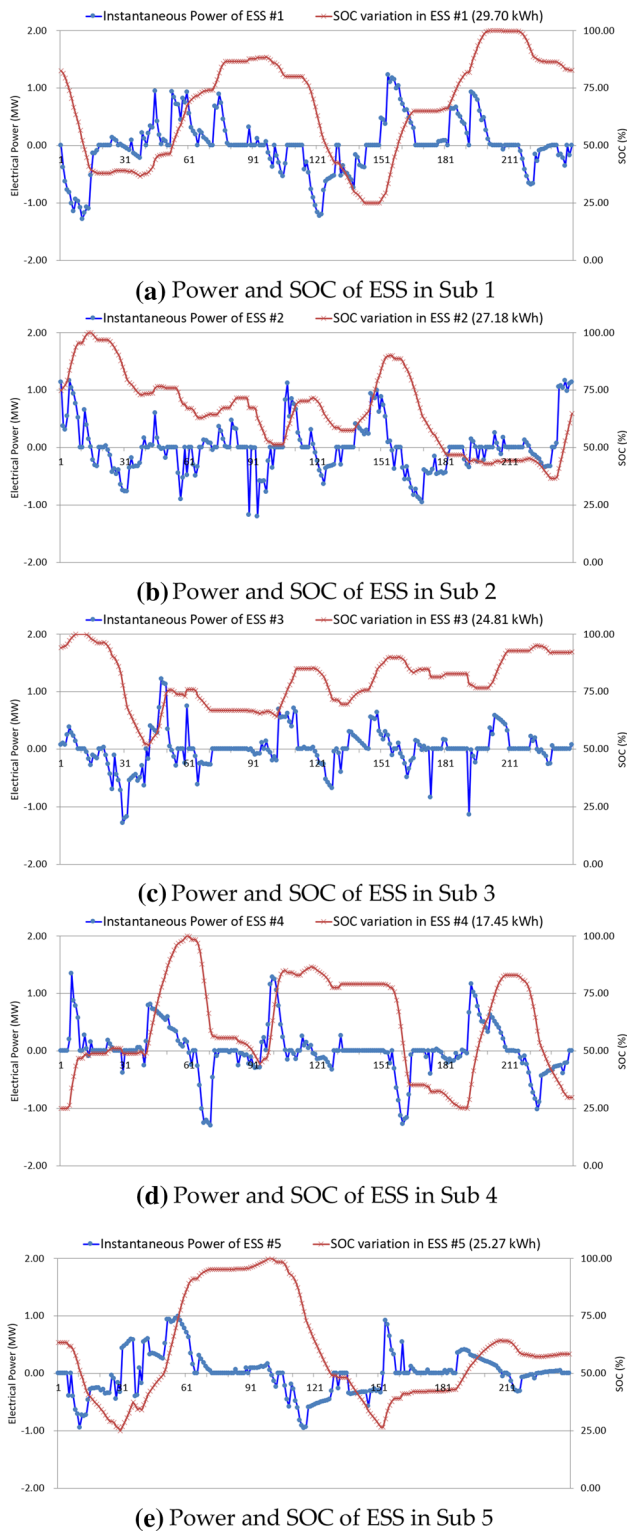


**Fig. 4** Power and SOC variation in peak headway condition

**Table 4** Optimal initial-SOC for off-peak headway condition

ESS location	Optimal initial SOC (%)
Sub 1	92.65
Sub 2	87.17
Sub 3	79.78
Sub 4	28.89
Sub 5	81.44

### 3.5 Discussions

The method proposed in this paper aims to solve the excess or shortage of storage capacity through appropriate selection of the initial charging amount, and this has been sufficiently proven through case studies. Also, as shown in Table 5, this shows not only the optimization of the storage capacity of each stationary ESS but also the energy exchange between ESSs. In the case of some ESSs, the instantaneous capacity required for charging and discharging increased, but overall, the capacity required for power conversion did not increase significantly. It should be noted that each storage capacity has been significantly decreased, and this is the result of considering the excess or shortage of capacity of nearby ESSs.

### 4 Conclusion

For the advanced applications of stationary ESSs as a means to increase energy efficiency in DC urban rail systems, an optimization algorithm has been proposed to determine the optimal power and storage capacity and the initial SOC level of ESSs in the railway substations. The proposed algorithm based on PSO is designed to estimate the available capacity and initial SOC in consideration of the missing capacity caused by storage capacity limits, the missing capacities of the nearby ESSs, and the electrical distance with them, so it has the strength of high convergence. In the case study based on the electrical, structural, and operational data of the actual route, it is verified that not only optimal design but also optimal operation is possible by utilizing the entire available range or minimizing DOD through the proposed algorithm. Based on this study, it is expected that advanced research on operational efficiency improvement, capacity optimization, and economic analysis based on the energy data network between ESSs will be achieved.

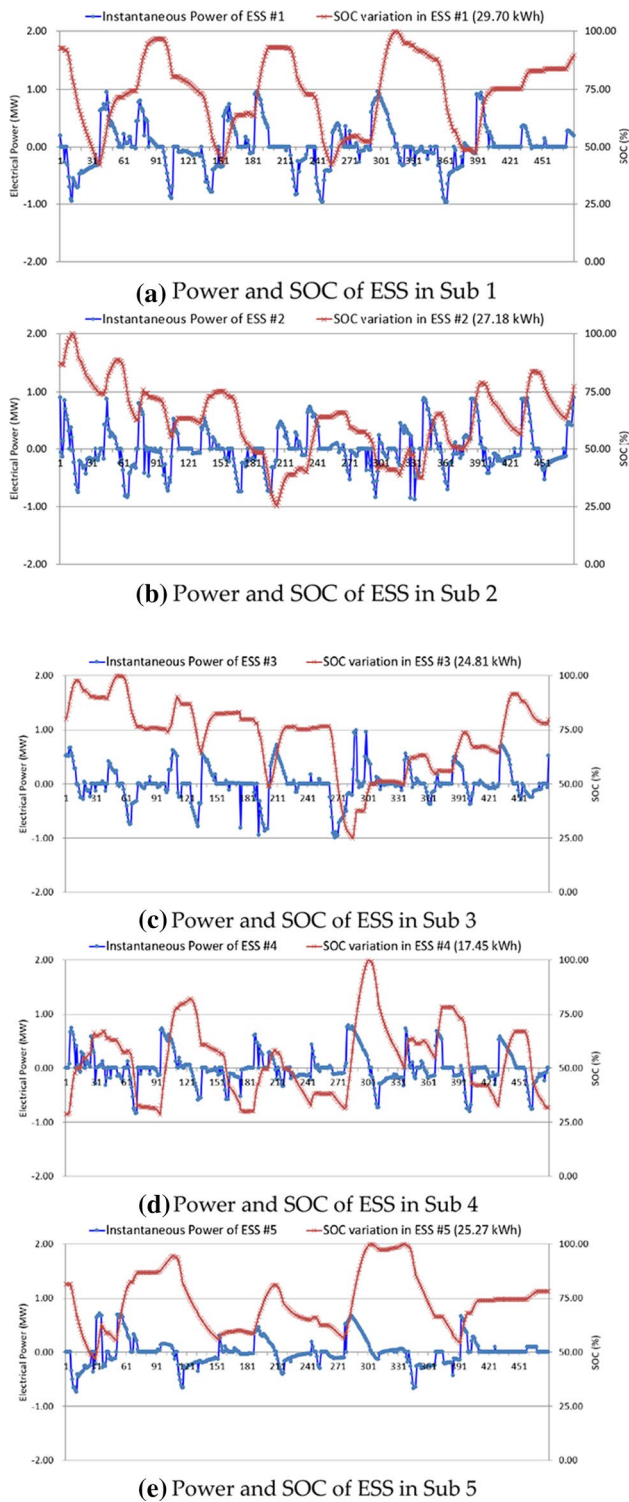


**Fig. 5** Power and SOC variation in off-peak headway condition

**Table 5** Comparison with the previous research

ESS location	Power capacity (MW)		Storage capacity(kWh)		storage capacity saving rate(%)
	Previous research (kWh)	This research (kWh)	Previous research (kWh)	This research	
Sub 1	1.293	1.283	31.20	29.70	95.19
Sub 2	1.148	1.197	27.71	27.18	98.10
Sub 3	1.351	1.279	31.20	24.81	79.52
Sub 4	1.102	1.345	19.00	17.45	91.84
Sub 5	1.013	0.993	27.01	25.27	93.55

**Acknowledgments** This research was funded by the Ministry of Land, Infrastructure and Transport’s Railway Technology Research Project, “Development of Real Time Simulator and Analysis Model for Railway Power System (21RTRP-B146034-04)”.

## References

- Bludszweit H, Dominguez-Navarro JA (2011) A probabilistic method for energy storage sizing based on wind power forecast uncertainty. *IEEE Trans Power Syst* 26(3):1651–1658
- Liu Y, Du W, Xiao L, Wang H, Bu S, Cao J (2016) Sizing a hybrid energy storage system for maintaining power balance of an isolated system with high penetration of wind generation. *IEEE Trans Power Syst* 31(4):3267–3275
- Schaltz E, Khaligh A, Rasmussen PO (2009) Influence of battery/ultracapacitor energy-storage sizing on battery lifetime in a fuel cell hybrid electric vehicle. *IEEE Trans Veh Technol* 58(8):3882–3891
- Akram U, Khalid M, Shafiq S (2018) Optimal sizing of a wind/solar/battery hybrid grid-connected microgrid system. *IET Renew Power Gener* 12(1):72–80
- Khorramdel H, Aghaei J, Khorramdel B, Siano P (2016) Optimal battery sizing in microgrids using probabilistic unit commitment. *IEEE Trans Industr Inf* 12(2):834–843
- Sharma S, Bhattacharjee S, Bhattacharya A (2016) Grey wolf optimisation for optimal sizing of battery energy storage device to minimise operation cost of microgrid. *IET Gener Transm Distrib* 10(3):625–637
- Shaghayegh B, Reder W, Khodaei A (2012) Reliability-constrained optimal sizing of energy storage system in a microgrid. *IEEE Trans Smart Grid* 3(4):2056–2062
- Lee H, Lee H, Lee C, Jang G, Kim G (2010) Energy storage application strategy on dc electric railroad system using a novel railroad analysis algorithm. *J Electr Eng Technol* 5(2):228–238
- Kim J, Kim J, Lee C, Kim G, Lee H, Lee B (2018) Optimal capacity estimation method of the energy storage mounted on the wireless railway train for energy-sustainable transportation. *Energies* 11(4):986
- Kim J, Ryu J, Kim G, Lee J, Chang S, Lee C, Kim J, Yongkuk Oh, Lee H, Kim J (2020) A proposed fast charging and high power



system for wireless railway trains adopting the input voltage sharing topology and the balancing control scheme. *IEEE Trans Ind Electron* 67(8):6407–6417

11. Lee H, Joo S-K, Jang G (2020) CDF-based capacity estimation method for stationary regenerative solution in parallel-fed DC urban subway transit. *IEEE Trans Sustain Energy* 11(1):206–216
12. Lee H, Song J, Lee H, Lee C, Jang G, Kim G (2012) Capacity optimization of the supercapacitor energy storages on DC railway system using a railway powerflow algorithm. *Int J Innov Comput Inf Control* 7(5):2739–2753
13. Lee H, Jung S, Cho Y, Yoon D, Jang G (2013) Peak power reduction and energy efficiency improvement with the superconducting flywheel energy storage in electric railway system. *Physica C - Supercond Appl* 494:246–249
14. Sengor I, Cilickiran HC, Akdemir H, Kekezoglu B, Erdinc O, Catalao JPS (2018) Energy management of a smart railway station considering regenerative braking and stochastic behaviour of ESS and PV generation. *IEEE Trans Sustain Energy* 9(3):1041–1050
15. Alfieri L, Battistelli L, Pagano M (2018) Energy efficiency strategies for railway application: alternative solutions applied to a real case study. *IET Electr Syst Transp* 8(2):122–129

**Publisher's Note** Springer Nature remains neutral with regard to jurisdictional claims in published maps and institutional affiliations.



**Kisuk Kim** received the B.S. Degree in electrical engineering from Soong-sil University, Seoul, Korea in 2010 and the M.S. and Ph. D degree from Korea University, Seoul, Korea in 2013 and 2018, respectively. He joined Korea Energy Agency (KEA), Ulsan, South Korea, in 2021. He is currently an assistant manager. His research interests include energy storage application in electric railway system and real-time digital simulation in power system.



**Jaewon Kim** received the B.S., M.S. and Ph.D. degrees in electrical engineering from Korea University, Seoul, South Korea, in 2006, 2008, and 2018, respectively. He joined Korea Railroad Research Institute (KRRI), Uiwang, South Korea, in 2011. He is currently a Senior Researcher with KRRI. His research interests include onboard energy storage system for railway trains, traction power supply system analysis and design, and railway electric components reliability analysis.



**Changmu Lee** received the M.S. degree in electronic communication engineering from Hanyang University, Seoul, South Korea, in 1993, and Ph.D. degree in electrical engineering from Korea University, Seoul, South Korea, in 2013. He is currently a Principal Researcher with Korea Railroad Research Institute (KRRI), Uiwang, South Korea. His research interests include electric railway system analysis and design.



**Joorak Kim** received the B.S., M.S. and Ph.D. degrees in electrical engineering from Hongik University, Seoul, South Korea, in 1997, 1999, and 2010, respectively. He is currently a Principal Researcher with Korea Railroad Research Institute (KRRI), Uiwang, South Korea. His research interests include static and dynamic analysis of traction power supply system.



**Hansang Lee** received the B.S., M.S. and Ph.D. degrees in electrical engineering from Korea University, Seoul, South Korea, in 2003, 2005, and 2010, respectively. He was a Research Professor with the School of Electrical Engineering, Korea University, Seoul, South Korea, from 2010.09 to 2012.02 and from 2017.03 to 2018.08. And he was an Assistant Professor with the School of Electrical & Railway Engineering, Kyungil University, Gyeongsan, South Korea, from 2012.03 to 2017.02. He is currently

Assistant Professor with the Department of Electrical Engineering, Semyung University, Jecheon, South Korea. His research interests include power and energy management in power system, energy storage application, electro-magnetic transient analysis, and electric railway system.